Band 32 (1996), S. 137–149

ZEITSCHRIFT FÜR
GLETSCHERKUNDE
UND GLAZIALGEOLOGIE

RECONSTRUCTION OF THE SUMMER MASS BALANCE OF HINTEREISFERNER SINCE 1953

By S. HOFINGER and M. KUHN, Innsbruck

With 6 figures

ABSTRACT

Annual mass balances of Hintereisferner have been determined since 43 years without distinction of seasonal balances. In order to evaluate summer mass balances an energy balance model was designed that is driven by the climate data of the nearest valley station. This model emphasizes short wave radiation fluxes and albedo in particular. Winter balances are evaluated as residuals of the annual balances.

REKONSTRUKTION DER SOMMERBILANZ DES HINTEREISFERNERS SEIT 1952/53

ZUSAMMENFASSUNG

Die jährliche Massenbilanz des Hintereisferners wird seit 43 Jahren mit der direkten glaziologischen Methode bestimmt, ohne daß dabei jahreszeitliche Bilanzen ausgesondert werden. Um die Sommerbilanzen zu berechnen, wurde ein Energiebilanzmodell erstellt, das mit den Klimadaten der nächsten Talstation betrieben wird. Dabei werden die Albedo und die kurzwelligen Strahlungsflüsse besonders berücksichtigt. Die Winterbilanzen werden als Restglied der Bilanz berechnet.

INTRODUCTION

Since 1952/53 the mass balance of Hintereisferner has been determined with the direct glaciological Method from annual measurements at the beginning of October (Hoinkes 1970). While a dense stake network was laid out in the first years, separate summer and winter balances were never evaluated. In the present paper we estimate annual summer balances with an energy balance model that uses climate data from Vent and parametrization schemes that were developed in a thesis by Hofinger (1994) on the basis of earlier studies. The meteorological station in Vent lies about 10 km downvalley from Hintereisferner at an altitude of 1890 m.

The calculations are based on a digital elevation model established from the map of Hintereisferner of 1979 (Kuhn 1979b) with a grid point distance of 50 m. This model is shown in figure 1.

The ablation zone of HEF is rather flat with a northeasterly aspect. Above the mean equilibrium line at 2960 m the accumulation area extends into slopes of various orientations and gradients up to the peak of Weißkugel at 3739 m.

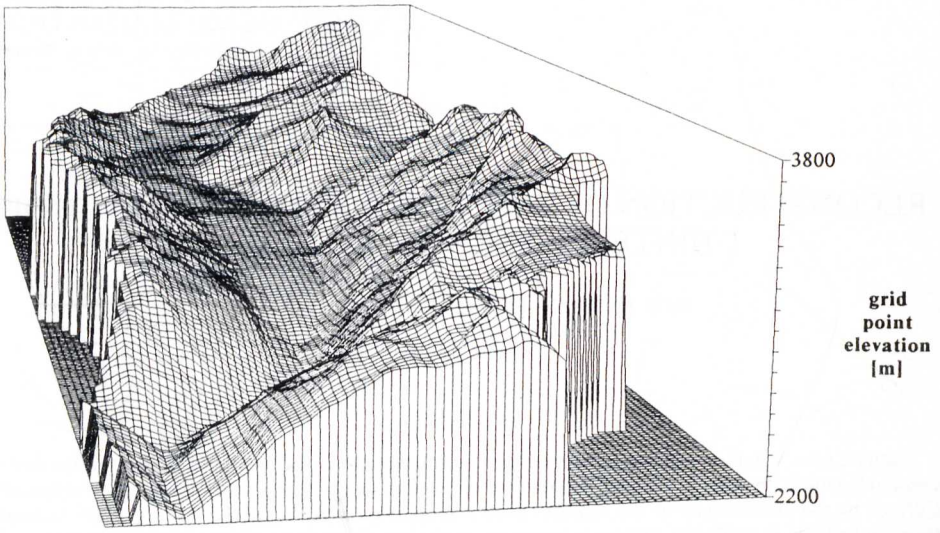

Fig. 1: Digital elevation model of Hintereisferner 1979, looking from NE towards Weißkugel (3739 m a.s.l.). Grid point distance is 50 m. From Hofinger (1994).

THE ENERGY BALANCE MODEL

The energy balance model that is summarized here is based on the experience of previous investigators at the Institute of Meteorology and Geophysics in Innsbruck (Hoinkes, Howorka and Schneider 1968, Wendler 1967, Hoinkes 1970, Dreiseitl 1977, 1978, 1980, Markl and Wagner 1978, Wagner 1979, 1980, Hoinkes and Steinacker 1975, Kuhn 1979a, 1981, 1984, 1987, Kuhn, Nickus, Pellet 1982, Kaser 1980, 1984) and has been described in detail by Hofinger (1994).

In the formal treatment of the energy balance we have chosen a sign convention that treats all energy gains as positive and gives a negative sign to all losses, i.e

$$F_R + F_H + F_L + F_G + F_M = 0$$

where the indices R, H, L, G, M, respectively denote radiation balance, sensible and latent heat, heat conduction and heat of fusion, the latter being negative in the case of melting. F_G and F_M are mutually exclusive, i.e. snow and ice can either change temperature or phase, and during the ablation season F_G is generally negligible compared to the other terms. The climatic variables and the boundary conditions derived from observations are summarized in fig. 2.

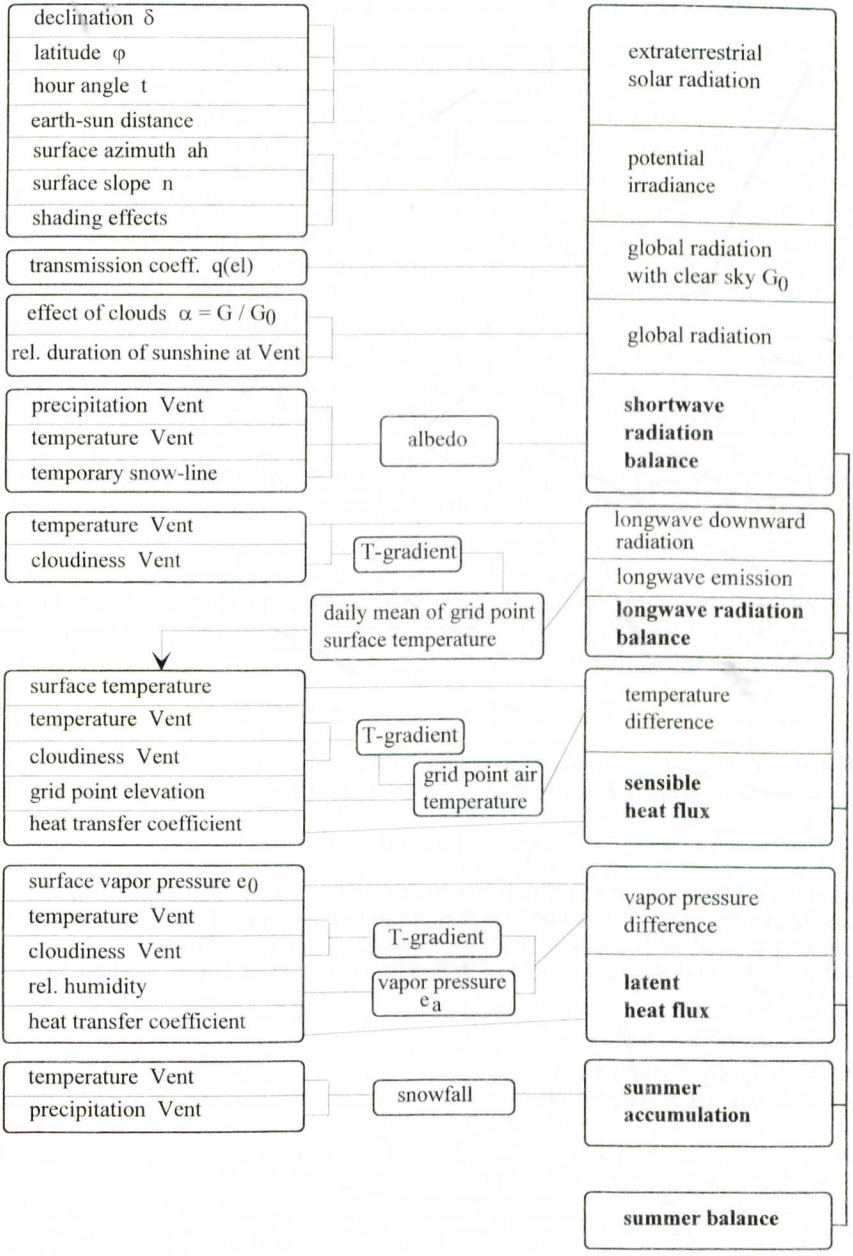

Fig. 2: Schematic summary of the energy balance model. Climatic variables and boundary conditions derived from observations given in the left column serve as input, intermediate results and computational steps appear in the center column while derived variables and energy balance terms are listed at the right side.

GLOBAL SHORTWAVE IRRADIANCE

The solar energy incident on the glacier surface is the primary forcing function in the energy balance. For the present purpose the shortwave radiation is computed in five steps that require 12 input variables according to fig. 2. The algorithms adopted here are similar to those used by Funk (1985), Escher-Vetter (1980) or Enders (1979), particularly for the first and second step that involve only astronomical and topographical input.

From the latitude, from daily values of solar declination and Earth to Sun distance, and from the solar hour angle the extraterrestrial solar irradiance of a horizontal unit area is determined as a first step. Next, the elevation angle of the mountains as seen from each grid point is evaluated for 10° azimuth sectors between +125° and –125°. For each time step the solar elevation is compared to the elevation of the mountain sky line in order to determine the times of sunrise and sunset at a particular grid point. A potential irradiance B is then calculated as reference by integrating all values of extraterrestrial irradiance over time from sunrise to sunset. All subsequent calculations proceed on the basis of these daily values.

From measurements of global irradiance G at Hintereis Station (3030 m a.s.l.) from 1979 to 1982 daily ratios of global to potential irradiance

$$q = G/B$$

were determined. For clear sky summer days the mean value q = 0.79 was found. Following Kuhn (1979a) global irradiance was assumed to increase with increasing gridpoint elevation by one percent per 100 m so that

$$q(z) = 0.79\ (1 + 0.01(z - 3000)/100))$$

The effect of clouds was parameterized with values of relative sunshine duration s at the station of Vent following Schram & Thams (1970), Rott (1974) and Kuhn (1984):

$$G = G(0)\ (\alpha + (1-\alpha)\sqrt{s}\ )$$

where α is the ratio of global irradiance under overcast sky to that under clear sky. From the monthly values of α given in table 1 a seasonal weighted mean of 0.43 is found which is in excellent agreement with the value of 0.42 given for Sonnblick (3100 m) by Sauberer and Dirmhirn (1958) and the mean of the 1971 ablation period at Hintereisferner of 0.50 by Wagner (1980).

Table 1: Monthly means of the ratio of global irradiance under overcast sky to that under clear sky, α, and means of the global radiation, numbers of days and means of cloudiness at HEF 1979–1982

month	clear days			overcast days			$\alpha = G_{10}/G_0$
	W/m²	number	cloud.	W/m²	number	cloud.	
May	343	11	1.5	150	11	9.7	0.44
June	368	6	1.5	158	6	9.7	0.43
July	348	5	0.5	142	5	9.3	0.41
August	289	13	1.6	134	13	9.4	0.46
September	222	12	1.0	96	12	8.3	0.44
Σ	1570	47	1.2	680	47	9.3	0.43

EXTRAPOLATION OF TEMPERATURE TO THE GLACIER LEVEL

The temperature at the glacier level decides whether precipitation falls in the form of rain or snow which in turn is decisive for the surface albedo at a grid point. Before discussing albedo we therefore need to explain the way temperature is extrapolated from the valley station to higher altitudes. Steinacker (1983) and Braun (1985) summarized several conditions for the transition from wet to solid precipitation from which we adopted a temperature of 2 °C as the only criterion.

The vertical temperature gradient between Vent and Hintereisferner depends on the time of the year, the time of the day and the synoptic or local weather condition. In the present analysis we admitted two variables, viz. the months and cloudiness as an indication of the weather situation. Records of 1979–82 have been classified in table 2 where a systematic variation is evident: May and June have the highest values since that ist the time of the year when strong insolation favors superadiabatic lapse rates and the snow line is situated between the valley station and the glacier. In August and September there is a higher incidence of inversions that is most clearly seen in the low cloudiness class but persists in the other two classes as well. The high cloudiness class displays the highest lapse rates since both cloudiness and strong mixing are associated with synoptic disturbances.

Table 2: Monthly temperature gradients [°C/100m] on different conditions in cloudiness

cloudiness	0–3.3/10	3.4–6.6/10	6.7–10/10
May	–0.71	–0.75	–0.73
June	–0.75	–0.74	–0.71
July	–0.55	–0.66	–0.69
August	–0.50	–0.59	–0.63
September	–0.36	–0.53	–0.59
May – September	–0.53	–0.64	–0.68

SURFACE ALBEDO

On the basis of these temperature extrapolations the model makes the rain/snowfall decision for each gridpoint whenever preciptitation is recorded at the valley station. The second crucial decision for the surface albedo parametrization concerns the existence of snow (firn) or bare ice at the gridpoint. As a sufficient number of terrestrial or satellite images of the glacier surface are not available a rather crude calculation of the position of the temporary snow line is used that is obtained from two periods of intensive observations of the ablation stake network on Hintereisferner, based on 28 stakes from 1970 to 79 and 18 from 1984 to 92. The data are shown in fig. 3 with a quadratic fit

$$SL(d) = 2490 + 5.73\ d - 0.213\ d^2 \text{ (m a.s.l.)}$$

where d is the number of days elapsed since snow disappeared and ice ablation began at the terminus altitude of 2490 m. In the data set used the correlation of SL with d was r=0.93.

An exponential decrease of surface albedo with time is usually observed (e.g. Corps of Egineers 1956) and after some trial and error we adopted a procedure in which on days with snowfall albedo is set equal to 0.9, the day after precipitation stopped it is set equal to 0.75 and thereafter it decays as

$$a(n) = a_{min} + K\, e^{-n\,k}$$

where a_{min} is the is the value that is exponentially approached, n is the number of days after the snowfall, $K = 0.75 - a_{min}$ and k was found to be 0.12. From the work of Wagner (1979) we assumed 0.5 for a_{min}. Fig. 4 compares Wagner's albedo measurements with the values calculated in the model. For old ice a_{min} was assumed to be 0.28 in dark areas and 0.38 in clean areas.

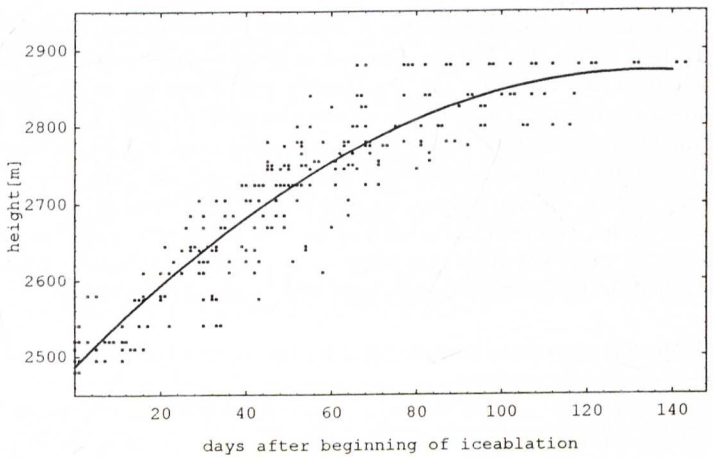

Fig. 3: Position of the transient snow line on Hintereisferner (in m a.s.l.) as function of time elapsed since the beginning of ice ablation at the terminus.

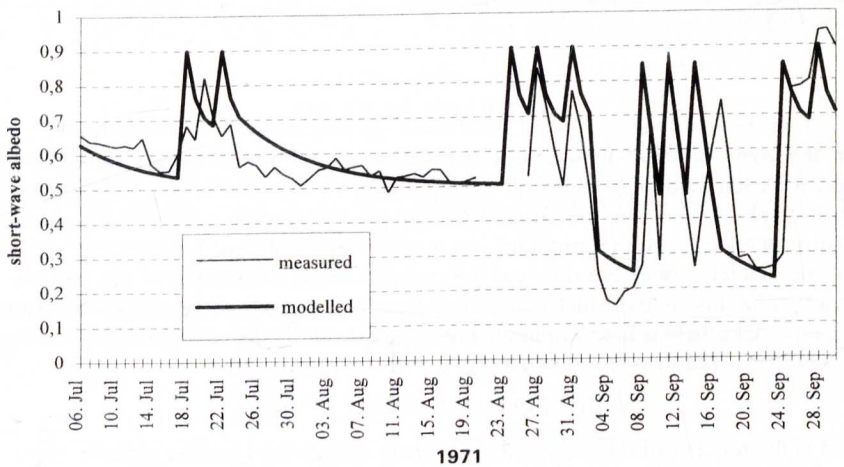

Fig. 4: The course of albedo at the equilibrium line of Hintereisferner (2960m) as measured in 1971 (Wagner 1979, thin line) and modelled in the present study (heavy line). In the course of the ablation period several snow falls restore high albedo values that tend to decay exponentially with time. At the beginning of September the transient snow line retreats past the measuring site, exposing old ice covered with patches of dark, fine material.

LONGWAVE RADIATION

The two most important atmospheric variables affecting longwave downward radiation are air temperature and vapor pressure. Lacking information on the distribution of vapor pressure over the entire glacier and having longwave measurements available only for the summer of 1971 we preferred to use the records of that summer for a multiple correlation of longwave downward irradiance with air temperature and the cloudiness observed at Vent. A correlation matrix was established for 11 classes of cloudiness and the temperature range from –5 to +15 °C which was used for the gridpoint temperatures and the cloud observations of Vent. A comparison of measured and modelled values is given in fig. 5. Müller (1984) has published a comprehensive collection of alpine longwave measurements.

The longwave emission from the glacier into the atmosphere was computed using Stefan and Boltzmann's law with unit emissivity.

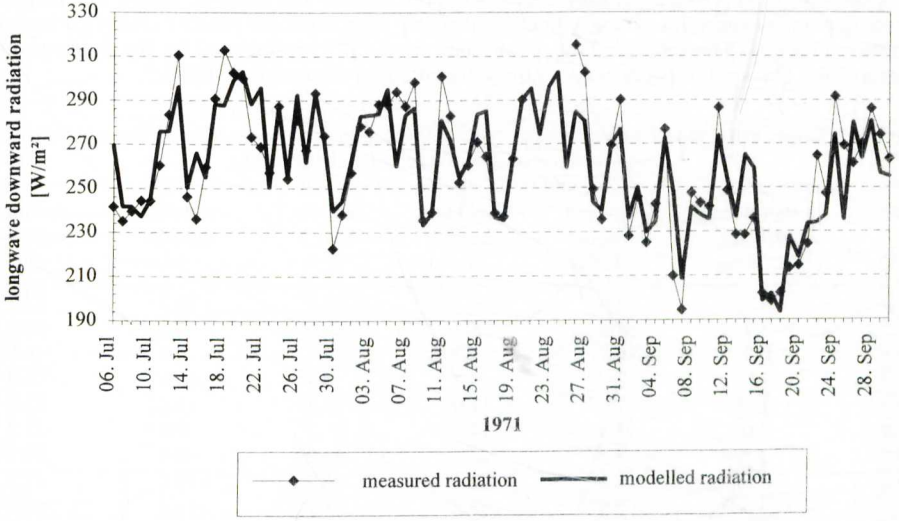

Fig. 5: Daily averages of longwave downward irradiance at Hintereisferner

TURBULENT FLUXES

For the parametrization of the sensible heat fluxes we chose the use of a bulk transfer coefficient α_H according to

$$F_H = \alpha_H (T_{air} - T_{sfce})$$

The value of α_H had been evaluated for Hintereisferner in an earlier study as 1.6 MJ $m^{-2}d^{-1}$ (Kuhn 1979a) but was reduced to 1.0 MJ $m^{-2}d^{-1}$ for smooth firn and to 1.25 MJ $m^{-2}d^{-1}$ for ice surfaces.

Latent heat fluxes were treated in a similar fashion assuming that a similar bulk transfer coefficient α_V is applicable (Kuhn 1984, 1987).

$$F_L = \alpha_V (e_{air} - e_{sfce})$$

While the values of the surface vapor pressure are identical with saturation vapor pressure at surface temperature we needed to make some strong assumptions in order to arrive at values for the vapor pressure in the boundary layer. We fixed the relative humidity at 50 % from 8 to 16 hours and to 80 % for the rest of the day all over the glacier and applied grid point temperatures two degrees below the daily mean for the night period and four degrees above the daily mean for the day period when evaluating the grid point vapor pressure. This procedure has introduced errors of up to 2 W m^{-2} when compared to actual measurements.

MODEL SENSITIVITY

In this model air temperature has a direct or indirect influence on all major energy balance components. It determines the transition from rain to snow fall and thereby albedo and the short wave radiation balance. Air temperature is direct input into the computation of sensible heat transfer and affects the latent heat computation via the saturation vapor pressure. Table 3 illustrates the effects of temperature changes in both relative and absolute terms. The response of the dependent variables is nearly linear and nearly symmetric for positive and negative temperature changes. The total amount of summer snow fall is influenced by the hypsographic curve of the glacier, but is linear to within ten percent in the range of Table 3.

Table 3: Changes in the model energy balance terms, modeled summer snow fall and summer balance, in response to prescribed temperature changes ΔT_a

ΔT_a	shortwave balance	longwave balance	sensible heat	latent heat	summer snowfall	summer balance
°C	%	%	%	%	%	%
–1.0	–4.9	–9.6	–36.7	–42.5	16.2	77.7
–0.5	–2.4	–4.5	–18.4	–21. 6	8.4	39.2
+0.1	0.5	0.9	3.7	4.4	–1.8	–8.0
+0.2	1.0	1.7	7.4	8.8	–3.6	–15.9
+0.3	1.5	2.6	11.0	13.2	–5.2	–23.8
+0.4	2.0	3.4	14.7	17 .7	–6.9	–31.8
+0.5	2.5	4.3	18.4	22.2	–8.4	–39.7
+0.6	3.0	5.1	22.1	26.7	–10.0	–47.7
+0.7	3.5	5.9	25.8	31.2	–11.6	–55.8
+0.8	4.0	6.7	2 9.5	35.8	–13.0	–63.9
+0.9	4.6	7.5	33.2	40.4	–14.7	–72.2
+1.0	5.1	8.3	36.9	45.0	–16.1	–80.6
	W/m^2	W/m^2	W/m^2	W/m^2	mm	mm
–1.0	–4	–6	–14	–10	+53	+983
–0.5	–2	–3	–7	–5	+28	+496
+0.1	0	0	+1	+1	–6	–101
+0.2	+1	+1	+3	+2	–12	–201
+0.3	+1	+1	+4	+3	–17	–301
+0.4	+2	+2	+6	+4	–23	–403
+0.5	+2	+2	+7	+5	–27	–502
+0.6	+3	+2	+8	+6	–33	–603
+0.7	+4	+3	+10	+7	–38	–705
+0.8	+4	+3	+11	+8	–43	–808
+0.9	+5	+4	+13	+9	–48	–913
+1.0	+6	+4	+14	+10	–53	–1020

The response of the model to changes in precipitation, lapse rate, heat transfer coefficient and albedo is summarized in Table 4. In order to give these sensitivities the appropriate weight, the changes in input have to be compared to the respective variances. This can be appreciated from the temperature gradients in Table 2 and from the respective standard deviations of summer mean temperature (± 0.8 K) and winter precipitation (± 210 mm or 25 %), both at 3000 m near Hintereisferner (Kuhn 1981).

Table 4: Changes in the model energy balance terms, modeled summer snow fall and summer balance, in response to prescribed changes of the lapse rate Δgrad, of the summer precipitation Δprec, of the heat transfer coefficient $\Delta\alpha_H$ and of the albedo Δa

Δgrad °C/100m	shortwave balance W/m²	longwave balance W/m²	sensible heat W/m²	latent heat W/m²	summer snowfall mm	summer balance mm
+0.05	+3	+2	+8	+5	–32	–476
+0.10	+6	+4	+16	+11	–61	–976
+0.15	+9	+7	+23	+17	–88	–1486
–0.05	–2	–3	–8	–6	+32	+464
–0.10	–4	–6	–16	–11	+61	+904
–0.15	–6	–9	–23	–16	+91	+1344
Δprec	W/m²	W/m²	W/m²	W/m²	mm	mm
+10.0	–0.1	0	0.0	0.0	+33	+33
+20.0	–0.2	0	+0.1	0.0	+66	+66
+30.0	–0.3	0	+0.1	+0.1	+98	+98
–10.0	+0.2	0	0.0	0.0	–33	–33
–20.0	+0.4	0	–0.1	0.0	–66	–66
–30.0	+0.5	0	–0.1	–0.1	–98	–98
$\Delta\alpha_H$	W/m²	W/m²	W/m²	W/m²	mm	mm
+0.1	0	0	+3	–3	0	+24
+0.2	0	0	+7	–5	0	+54
–0.1	0	0	–3	+1	0	–26
–0.2	0	0	–7	+3	0	–56
Δ Alb	W/m²	W/m²	W/m²	W/m²	mm	mm
+0.01	–2	0	0	0	0	+54
+0.02	–4	0	0	0	0	+124
+0.03	–6	0	0	0	0	+184
+0.05	–11	0	0	0	0	+304

RESULTS

In order to check the reliability or plausibility of the computed ablation rates and summer balances a number of frequently controlled ablation stakes were selected and compared with the ablation modelled for the nearest grid points as shown in Table 5. While this comparison is very encouraging as far as the ablation area is concerned, less confidence can be given to the results in the accumulation area. While the model calculates summer precipitation as function of temperature and thereby indirectly as function of altitude, wind and avalanches redistribute precipitation on the real glacier. Plots of both calculated summer precipitation and summer balance reflect these shortcomings, but we argue that summer

snow is far less mobile than cold, dry winter snow and that in summer the effects of redistribution by drift and avalanches cancel when integrated over the entire glacier area.

Table 5: Measured and calculated ablation at selected stakes

ablation stake	measured [m w.eq.]	calculated [m w.eq.]	difference [m w.eq.]	deviation %
22	2.25	2.22	–0.03	–1
27	0.92	0.91	–0.01	–1
28	0.94	0.92	–0.02	–2
31	0.56	0.58	0.02	4
32	0.40	0.41	0.01	2
72	4.78	4 .55	–0.23	–5
76	4.20	4.00	–0.20	–5
77	3.18	3.63	0.45	14
81	4.32	4.30	–0.02	–0.5

Table 6 and fig. 6 summarize the results as a 43 years time series of summer, winter and annual balances. Values of the summer balances reach minima below in four years and were positive in only two years. The mean summer balance is –1060 mm w.e. with a standard deviation of ± 660 mm.

Table 6: Mass balance components of Hintereisferner. The annual balances were determined with the direct glaciological method, the summer balances were modeled and the winter balances are residuals

balance year	annual balance	winter balance	summer balance	balance year	annual balance	winter balance	summer balance
1952/53	–540	700	–1240	1974/75	70	1010	–940
1953/54	–290	–70	–220	1975/76	–310	410	–720
1954/55	80	190	–110	1976/77	760	1030	–270
1955/56	–280	370	–650	1977/78	410	790	–380
1956/57	–190	130	–320	1978/79	–220	450	–670
1957/58	–980	490	–1470	1979/80	–50	930	–980
1958/59	–760	550	–1310	1980/81	–170	830	–1000
1959/60	–60	230	–290	1981/82	–1240	710	–1950
1960/61	–210	1610	–1820	1982/83	–580	1740	–2320
1961/62	–700	370	–1070	1983/84	–30	870	–840
1962/63	–600	530	–1130	1984/85	–570	1200	–1770
1963/64	–1250	570	–1820	1985/86	–730	1090	–1820
1964/65	9 30	590	340	1986/87	–720	1090	–1810
1965/66	340	790	–450	1987/88	–980	640	–1620
1966/67	20	900	–880	1988/89	–640	350	–990
1967/68	340	310	30	1989/90	–1000	370	–1370
1968/69	–430	290	–720	1990/91	–1330	990	–2320
1969/70	–550	430	–980	1991/92	–1120	970	–2090
1970/71	–600	550	–1150	992/93	–570	700	–1270
1971/72	–70	310	–380	1993/94	–1110	890	–2000
1972/73	–1230	560	–1790	1994/95	–400	780	–1180
1973/74	60	790	–730				
				mean	–390	670	–1060
				σ	540	370	660

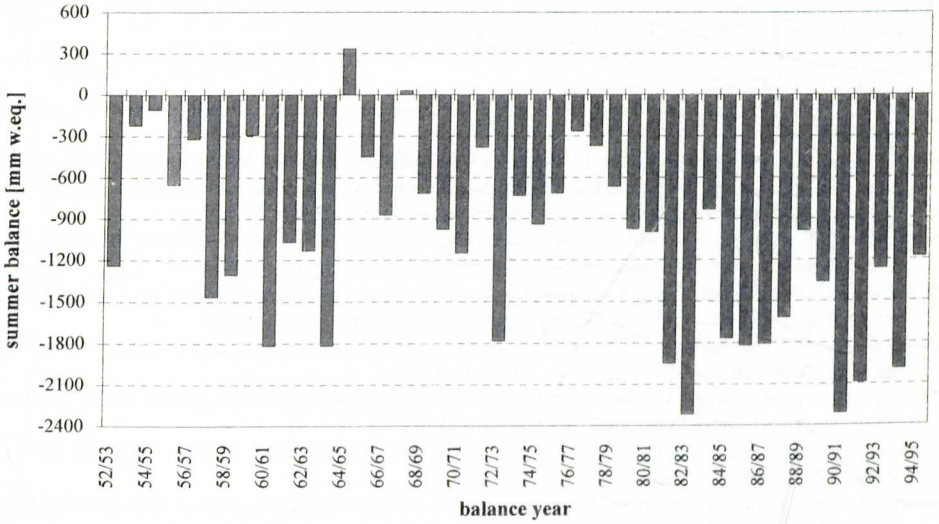

Fig. 6: The time series of mean specific summer balances of Hintereisferner, 1952/53 to 1994/95. (2960 m a.s.l.). Modelled values compared with measurements by Wagner (1980).

The residual obtained when subtracting the modelled summer balance from the measured annual balance was called ‚winter balance'. It has to absorb all errors and simplifications introduced by measurements and model calculations, but the low standard deviation of this residual indicates that errors are low and tolerable. While the balances of the first year of the series match very well with those of 1992/93, the annual balances of some of the following, early years may be in error and produce conspicuous winter balances. We would expect the winter balance to be at least equal to the winter precipitation recorded at Vent for these years. The exceptional winter balance of 1982/83, however, is confirmed by precipitation records.

In view of the fact that the summer balance has a higher standard deviation in absolute values (± 540 mm) than winter balance (± 370 mm) we agree with Hoinkes (1970) who emphasized that the annual balance is determined by summer snow falls and associated albedo changes.

ACKNOWLEDGEMENT

This study was supported by the Austrian National Committee for the IGBP at the Austrian Academy of Sciences.

REFERENCES

Braun, L. N., 1985: Simulation of Snowmelt-Runoff in Lowland and Lower Alpine Regions of Switzerland. Züricher Geographische Schriften 21, 166 pp., ETH Zürich.

Corps of Engineers, 1956: Snow Hydrology. US Army North Pacific Division corps of Engineers, Portland, Oregon, 437 pp.

Dreiseitl, E., 1977: Zur Berechnung der Eisablation. Zeitschrift für Gletscherkunde und Glazialgeologie XII (1): 75–78.

Dreiseitl, E., 1978: Witterungsklimatologie von Vent und Massenbilanz des Hintereisferners. Arbeiten aus der Zentralanstalt für Meteorologie und Geodynamik 31: 57/1–5.

Dreiseitl, E., 1980: Mass balance of glaciers and general circulation. Materialyi Glatsiologicheskikh issledovanii 38: 187–196.

Enders, G., 1979: Theoretische Topoklimatologie. Forschungsberichte des Nationalparks Berchtesgaden 1/1979, 92 pp.

Escher-Vetter, H., 1980: Der Strahlungshaushalt des Vernagtferners als Basis der Energiehaushaltsberechnung zur Bestimmung der Schmelzwasserproduktion eines Alpengletschers. Wissenschaftliche Mitteilungen des Meteorologischen Instituts der Universität München No. 39, 115 pp.

Funk, M., 1985: Räumliche Verteilkung der Massenbilanz auf dem Rhonegletscher und ihre Beziehung zu Klimaelementen. Züricher Geographische Schriften No. 24, 183 pp.

Hofinger, St., 1994: Modellierung der Sommerbilanzen des Hintereisferners zwischen 1952 und 93. Thesis, Institute of Meteorology and Geophysics, University of Innsbruck, 133 pp.

Hoinkes, H., 1970: Methoden und Möglichkeiten von Massenhaushaltsstudien auf Gletschern. Zeitschrift für Gletscherkunde und Glazialgeologie VI(1): 37–90.

Hoinkes, H, F. Howorka and W. Schneider: Glacier mass budget and mesoscale waether in the Austrian Alps 1964 to 66. IAHS Publication No. 79: 241–254.

Hoinkes, H. und R. Steinacker, 1975: Zur Parametrisierung der Beziehung Klima – Gletscher. Rivista Italiana di Geofisica 1: 97–104.

Kaser, G., 1980: Measurements of evaporation from snow. Archiv für Meteorologie, Geophysik und Bioklimatologie, Serie B, 30: 333–340.

Kaser. G., 1984: Über die Verdunstung auf dem Hintereisferner. Zeitschrift für Gletscherkunde und Glazialgeologie 19(2): 149–162.

Kuhn, M., 1979a: On the computation of heat transfer coefficients from energy balance gradients. Journal of Glaciology 22(87): 263–272.

Kuhn, M., 1979b: Begleitworte zur Karte des Hintereisferners 1979, 1:10000. Zeitschrift für Gletscherkunde und Glazialgeologie 16(1): 117–124.

Kuhn, M., 1981: Climate and glaciers. IAHS Publication no. 131: 3–20.

Kuhn, M., 1984: Physikalische Grundlagen des Energie- und Massenhaushalts der Schneedecke. Mitteilungen des Deutschen Verbandes für Wasserwirtschaft und Kulturbau, Heft 7: 5–56.

Kuhn, M., 1987: Micro-meteorological conditions for snow melt. Journal of Glaciology 33(113): 24–26.

Kuhn, M., U. Nickus und F. Pellet 1982: Die Niederschlagsverhältnisse im inneren Ötztal. 17. Internationale Tagung für Alpine Meteorologie, Berchtesgaden 1982. Deutscher Wetterdienst, Offenbach, p. 235–239.

Markl, G. and H.-P. Wagner, 1978: Messungen von Eis- und Firntemperaturen am Hintereisferner. Zeitschrift für Gletscherkunde und Glazialgeologie 13(1/2): 261–265.

Müller, H., 1984: Zum Strahlungshaushalt im Alpenraum. Mitteilungen der Versuchsanstalt für Wasserbau, Hydrologie und Glaziologie, ETH Zürich, No. 71, 167 pp.

Rott, H., 1974: Sonnenschein, Globalstrahlung und Lufttrübung in Innsbruck. Ph.D. thesis, Institute of Meterology and Geophysics, University of Innsbruck, 191 pp.

Sauberer, F., and I. Dirmhirn, 1958: Das Strahlungsklima. Klimatographie von Österreich., Edited by F. Steinhauser, O. Eckel, F. Lauscher. Austrian Academy of Sciences, Denkschrift der Gesamtakademie 3(1): 13–102.

Schram, K. and J. C. Thams, 1970: Die kurzwellige Globalstrahlung und die diffuse Himmelsstrahlung am Flugplatz Zürich-Kloten. Publications of the Swiss Meteorological Agency No. 16, 23 pp.

Steinacker, R., 1983: Diagnose und Prognose der Schneefallgrenze. Wetter und Leben 35: 81–90.

Wagner, H.-P., 1979: Strahlungshaushaltsuntersuchungen an einem Ostalpengletscher während der Hauptablationsperiode. Teil 1, Kurzwellige Strahlung. Archiv für Meteorologie, Geophysik und Bioklimatologie, Serie B, 27: 297–324.

Wagner, H.-P., 1980: Strahlungshaushaltsuntersuchungen an einem Ostalpengletscher während der Hauptablationsperiode. Teil 2, Langwellige Strahlung und Strahlungsbilanz. Archiv für Meteorologie, Geophysik und Bioklimatologie, Serie B, 28: 41–62.

Wendler, G., 1967: Die Vergletscherung in Abhängigkeit von Exposition und Höhe und der Gebietsniederschlag im Einzugsgebiet des Pegels Vent in Tirol. Archiv für Meteorologie, Geophysik und Bioklimatologie, Serie B, 15: 260–273.

Manuscript received October 20, 1994, revised June 12, 1996.

Authors' address: Stefan Hofinger
Michael Kuhn
Institut für Meteorologie und Geophysik
Innrain 52
A-6020 Innsbruck, Austria
meteorologie @uibk.ac.at